Depth-Averaged Modelling of Erosion and Sediment Transport in Free-Surface Flows

Thomas Rowan, Mohammed Seaid

Abstract—A fast finite volume solver for multi-layered shallow water flows with mass exchange and an erodible bed is developed. This enables the user to solve a number of complex sediment-based problems including (but not limited to), dam-break over an erodible bed, recirculation currents and bed evolution as well as levy and dyke failure. This research develops methodologies crucial to the under-standing of multi-sediment fluvial mechanics and waterway design. In this model mass exchange between the layers is allowed and, in contrast to previous models, sediment and fluid are able to transfer between layers. In the current study we use a two-step finite volume method to avoid the solution of the Riemann problem. Entrainment and deposition rates are calculated for the first time in a model of this nature. In the first step the governing equations are rewritten in a non-conservative form and the intermediate solutions are calculated using the method of characteristics. In the second stage, the numerical fluxes are reconstructed in conservative form and are used to calculate a solution that satisfies the conservation property. This method is found to be considerably faster than other comparative finite volume methods, it also exhibits good shock capturing. For most entrainment and deposition equations a bed level concentration factor is used. This leads to inaccuracies in both near bed level concentration and total scour. To account for diffusion, as no vertical velocities are calculated, a capacity limited diffusion coefficient is used. The additional advantage of this multilayer approach is that there is a variation (from single layer models) in bottom layer fluid velocity: this dramatically reduces erosion, which is often overestimated in simulations of this nature using single layer flows. The model is used to simulate a standard dam break. In the dam break simulation, as expected, the number of fluid layers utilised creates variation in the resultant bed profile, with more layers offering a higher deviation in fluid velocity . These results showed a marked variation in erosion profiles from standard models. The overall the model provides new insight into the problems presented at minimal computational cost.

Keywords—Erosion, finite volume method, sediment transport, shallow water equations.

I. INTRODUCTION

MODELLING of sediment transport has been one of the oldest challenges facing hydro-engineers, as sediment erosion and deposition often undermines or clogs up engineering works. Gaining accurate predictions for sedimentary flows is an ever evolving problem, studied by many researchers [17], [9], [22], with varying statistical or numerical fluid model based approaches. Numerical fluid based models for sediment transport have been around since before the advent of modern computing [10], [2], [6]. Though the pace of development was hugely aided by modern computing with the first uncoupled models for flow and sediment transport emerging around the 1970s and 80s. These models were limited as they could not take into account the

T. S. L. Rowan is with the Department of Engineering, Durham University, Co. Durham, UK (e-mail: thomas.rowan@durham.ac.uk).

M. Seaid is with the Department of Engineering, Durham University, Co. Durham, UK (e-mail: m.seaid@durham.ac.uk).

effects of the sediment on the fluid. Recent models [4], [5], [15], [16], [21], [24], [19] have coupled the equations of sediment transport and fluid flow to gain more accurate results, especially in high shear/sediment concentration situations like dam-break problems.

Much work has been done to account for the sediment distribution in [25], [14] amongst others. Some even utilise separate fractions for both bed (supported by the bed, moved by the fluid) and suspended (suspended and moved by the fluid) loads [12]. Whilst this approach often increases accuracy, it nonetheless involves complex load equations that slow simulations. Furthermore it does not represent the fluid flow in complex transport situations where wind and/or recirculation can affect sediment transport. With a review of the current literature the following appear clear:

1) Sediment transport models are tested against several benchmarks mostly dam-break situations over movable beds. Models often over-predict net erosion in dam-break situations, as the sediment pickup functions for depth averaged results often over-predict fluid velocity at bed level. No multilayer flow results are available.
2) A large proportion of models use linearized Roe solvers to deal with the Riemann problem with regards to fluxes. This method is much slower than the Finite Volume of Characteristics (FVC) method and offers little advantage in accuracy by comparison [1].
3) The methods developed by Meyer-Peter & Muller [20], Van Rijn [26] and Grass [11] are most widely used in sediment transport models, and although they are not the most recent they remain amongst the most popular. It should be noted that these sediment transport models often rely on inter-changeable sediment pick up and deposition functions for various different situations (cohesive and non-cohesive sediments, etc.)

In this study we aim to tackle the problems of sediment distribution in sedimentary flows, at the same time as gaining more accurate results for high shear erosion processes. To achieve this we utilize a fully coupled multilayer flow model with sediment transport. The model is an adaptation of one proposed and developed by Audusse et al. [1] and it is developed to include sediment transport, as most models used depth-averaged concentration to account for sediment flow. In this study we aim to surpass this assumption by allocating each layer of water its own depth-averaged concentration. A simple four-equation model, consisting of the shallow water equations for mass and momentum, a species conservation equation for concentration and a bed Exner equation is adapted

World Academy of Science, Engineering and Technology
International Journal of Mechanical and Mechatronics Engineering
Vol:11, No:10, 2017

for multilayer use, as detailed in the next section. The FVC method - as detailed in [3] - is used. This is achieved by estimating the fluxes using the method of characteristics in the predictor step and then recovering the fluxes to the conservative formulation in the corrector stage.

This paper is structured as follows: A brief overview of the governing equations considered in this study is given in Section II. A short review of the numerical methods used is outlined in Section III. In Section IV results of benchmark and novel testing are presented. Finally in Section V some conclusions are drawn.

II. GOVERNING EQUATIONS

We consider the system shown in Fig. 1, where the flow is divided into multiple layers. Each layer has its own velocity, height and concentration (varying with x). The system also includes the effects of wind, bed friction, friction and momentum exchange between the layers.
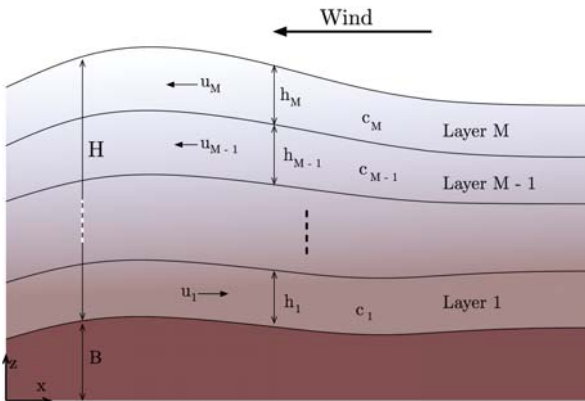

Fig. 1 A sketch of a multi-layered fluid system

To create a multi-layered system of equations we must first consider a single layer basic equations of momentum and mass conservation. To this end the 1D shallow water equations for a layer are derived from the Navier-Stokes as shown in (1) and (2). These equations are adapted to include the intra-layer forces alluded to earlier. Through integration of the one-dimensional form of the Navier-Stokes equations, and including terms for mass exchange, we arrive at:

$$\frac{\partial h_\alpha}{\partial t} + \frac{\partial}{\partial x}(h_\alpha u_\alpha) = G_{\alpha-1/2} - G_{\alpha+1/2}, \quad (1)$$

$$\frac{\partial (h_\alpha u_\alpha)}{\partial t} + \frac{\partial}{\partial x}\left(h_\alpha u_\alpha^2 + \frac{1}{2}gh_\alpha^2\right) = -gh_\alpha\frac{\partial B}{\partial x} + F_\alpha. \quad (2)$$

Through the summation of (1) across all the layers, and with the addition of a species conservation (for sediment) and a bed Exner equation, we arrive at the system of equations shown in (3). These equations are fully coupled for sediment transport, with the effects on momentum of sediment transport and scour and deposition included. We also add relevant terms for depth averaged concentration c, erosion E, and deposition D to the conservation and momentum equations. This gives us the governing equations:

$$\frac{\partial H}{\partial t} + \sum_{l=1}^{M}\frac{\partial}{\partial x}(h_\alpha u_\alpha) = \frac{E_1 - D_1}{1-p},$$

$$\frac{\partial (h_\alpha u_\alpha)}{\partial t} + \frac{\partial}{\partial x}\left(h_\alpha u_\alpha^2 + \frac{1}{2}gh_\alpha^2\right) = -gh_\alpha\frac{\partial B}{\partial x}$$

$$-\frac{(\rho_s - \rho_w)}{2\rho_\alpha}gh_\alpha^2\frac{\partial c_\alpha}{\partial x} - \frac{(\rho_s - \rho_w)}{2\rho_\alpha}gh_\alpha^2\frac{\partial c_\alpha}{\partial z}$$

$$-\frac{1}{l_\alpha}\Big(\frac{(\rho_0 - \rho_\alpha)(E_\alpha - D_\alpha)u}{\rho_\alpha(1-p)} + F_\alpha,$$

$$\frac{\partial(h_\alpha c_\alpha)}{\partial t} + \frac{\partial (h_\alpha u_\alpha c_\alpha)}{\partial x} = E_\alpha - D_\alpha$$

$$-c_{\alpha+1/2}G_{\alpha+1/2} + c_{\alpha-1/2}G_{\alpha-1/2} + \epsilon\frac{\partial^2 c_\Delta}{\partial z^2},$$

$$\frac{\partial B}{\partial t} = -\frac{E_1 - D_1}{1-p}$$

$$(3)$$

where ρ is the sediment fluid mixture density, ρ_s is the density of the sediment and ρ_w is the density of water. The water height h_l of the l layer is defined as:

$$h_\alpha = l_\alpha H, \quad \alpha = 1, ..., M. \quad (4)$$

The total number of fluid layers is M, and F_α is the sum of the external forces acting on the layer (wind, friction and momentum exchange effects). There are four components that make up F_α:

$$F_\alpha = F_u + F_b + F_w + F_\mu. \quad (5)$$

A. Intra-Layer Force Equations

F_u is the term for momentum exchange between layers as defined by:

$$F_u = u_{\alpha+1/2}G_{\alpha+1/2} - u_{\alpha-1/2}G_{\alpha-1/2} \quad (6)$$

the mass exchange between layers is:

$$G_{\alpha+1/2} = \sum_{\beta=1}^{l}\left(\frac{\partial(h_\beta u_\beta)}{\partial x} - l_\beta\sum_{\gamma=1}^{M}\frac{\partial h_\gamma u_\gamma}{\partial x}\right), \quad \alpha = 1, ..., M-1, \quad (7)$$

F_l is the term describing vertical kinematic eddy viscosity and calculates the friction between neighbouring layers, it is defined as:

$$F_\mu = \begin{cases} -2\nu\frac{u_{\alpha-1}-u_\alpha}{(l_{\alpha-1}+l_\alpha)H}, & \text{if } \alpha = M, \\ 2\nu\frac{u_{\alpha+1}-u_\alpha}{(l_{\alpha+1}+l_\alpha)H} - 2\nu\frac{u_{\alpha-1}-u_\alpha}{(l_{\alpha-1}+l_\alpha)H}, & \text{if } 2 \le \alpha \le M-1, \\ 2\nu\frac{u_{v+1}-u_l}{(l_{\alpha+1}+l_\alpha)H}, & \text{if } \alpha = 1, \end{cases} \quad (8)$$

ν is the eddy viscosity, the friction term between the bottom layer and the bed is described as:

$$F_b = \begin{cases} -\frac{gn_b^2}{H^{1/3}}u_1|u_1|, & \text{if } \alpha = 1, \\ 0, & \text{otherwise}, \end{cases} \quad (9)$$

World Academy of Science, Engineering and Technology
International Journal of Mechanical and Mechatronics Engineering
Vol:11, No:10, 2017

where n_b is the Manning roughness coefficient. The effect of the wind on the top layer is given by:

$$F_w = \begin{cases} -\frac{\sigma^2 \rho_a}{H} w|u_1 w|, & \text{if } \alpha = M, \\ 0, & \text{otherwise}, \end{cases} \qquad (10)$$

where w is the wind velocity (10m above the water surface) and σ is the wind stress coefficient.

B. Equations for Erosion and Deposition

We utilise the empirical relations as reported in [7], that assume a non-cohesive sediment:

$$D_\alpha = \begin{cases} w(1-C_a)^{1.4} C_a, & \text{if } \alpha = 1, \\ 0, & otherwise, \end{cases} \qquad (11)$$

w is the deposition coefficient as quantified by [27], [29], [23] amongst others, d is the average diameter of the sediment, m is an exponent indicating the effects of hindered settling due to high sediment concentrations, and C_a the near-bed volumetric sediment concentration. $C_a = \beta_c c_\alpha$, where β_c is a coefficient larger than unity. To stop the near bed concentration from exceeding $1 - p$ (its measured maximum) the exponent β_c is limited by (as in [8]):

$$\beta_c = \min\left(2, \frac{1-p}{c_\alpha}\right).$$

Erosion is defined as:

$$E_\alpha = \begin{cases} \varphi \frac{\theta - \theta_c}{h_1} u_1 d^{-0.2}, & \text{if } \theta \geq \theta_c \text{ and } \alpha = 1, \\ 0, & \text{otherwise}. \end{cases} \qquad (12)$$

C. Vertical Sediment Diffusion

As we have no vertical velocities calculated in this model, vertical sediment diffusion is a major problem for a system formulation of this type, thus we introduce a sediment diffusion coefficient ϵ_Δ. Huge effort has been undertaken to both measure [28] and compute [13], [14] the vertical diffusion of sediment in flows. Fig. 2 shows a typical sediment distribution in a turbulent flow.
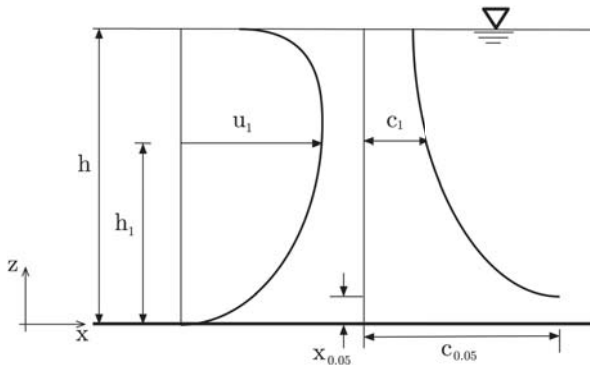

Fig. 2 A sketch of a typical sediment distribution as [18]

As we know the shape and for various measured sediments the precise sediment distribution, we propose a simple

method for vertical distribution. Rather than computationally expensively calculating the diffusion for each cell boundary we cap the amount of diffusion by comparing the sediment to be diffused to the portion that should be diffused. In this way we assume a distribution curve of, for example C_0, at say $C_0 = \frac{1}{z}$. Then by applying the limits we know for each layer α we gain

$$C_{0,\alpha} = \left(\frac{ln(z_{\alpha+\frac{1}{2}}) - ln(z_{\alpha-\frac{1}{2}})}{ln(h + \lambda_c) - ln(h_{0.05} + \lambda_c)}\right) \sum_{\alpha=1}^{M} (c_\alpha h_\alpha). \quad (13)$$

So we define the diffusible amount in a given layer as

$$c_{\Delta,\alpha+\frac{1}{2}} = \frac{1}{h_\alpha} \left(C_{0,\alpha+1} - c_{\alpha+1} h_{\alpha+1} - C_{0,\alpha} + c_\alpha h_\alpha\right). \quad (14)$$

This method is easily adaptable to any sediment distribution curve and, as the distribution curve can be calculated in advance of any time-stepping procedure, it is quick to implement.

III. Numerical Methods

For ease we re-arrange the governing equations in (3) into vector form:

$$\frac{\partial \mathbf{W}}{\partial t} + \frac{\partial \mathbf{F}(\mathbf{W})}{\partial x} = \mathbf{Q}(\mathbf{W}) + \mathbf{R}(\mathbf{W}), \qquad (15)$$

where $\mathbf{W}$ is the vector of conserved variables, $F(\mathbf{W})$ is the vector of flux functions, $\mathbf{Q}$ and $\mathbf{R}$ are the vectors of source terms.

$$\mathbf{W} = \begin{pmatrix} H \\ Hu_1 \\ Hc_1 \\ Hu_2 \\ Hc_2 \\ \vdots \\ Hu_M \\ Hc_M \\ B \end{pmatrix}, \mathbf{F}(\mathbf{W}) = \begin{pmatrix} \Sigma_{\alpha=1}^{M} l_\alpha Hu_\alpha \\ Hu_1^2 + \frac{1}{2}gH^2 \\ Hu_1 c_1 \\ Hu_2^2 + \frac{1}{2}gH^2 \\ Hu_2 c_2 \\ \vdots \\ Hu_M^2 + \frac{1}{2}gH^2 \\ Hu_M c_M \\ 0 \end{pmatrix},$$

$$\mathbf{Q}(\mathbf{W}) = \begin{pmatrix} 0 \\ -gh\frac{\partial Z}{\partial x} - \frac{(\rho_s - \rho_w)}{2\rho_1} gh^2 \frac{\partial c_1}{\partial x} \\ 0 \\ -gh\frac{\partial Z}{\partial x} - \frac{(\rho_s - \rho_w)}{2\rho_2} gh^2 \frac{\partial c_2}{\partial x} \\ 0 \\ \vdots \\ -gh\frac{\partial Z}{\partial x} - \frac{(\rho_s - \rho_w)}{2\rho_M} gh^2 \frac{\partial c_M}{\partial x} \\ 0 \\ 0 \end{pmatrix}, \quad (16)$$

World Academy of Science, Engineering and Technology
International Journal of Mechanical and Mechatronics Engineering
Vol:11, No:10, 2017

$$\mathbf{R}(\mathbf{W}) = \begin{pmatrix} \dfrac{E_1 - D_1}{1 - p} \\ -\dfrac{1}{l_1}(K_{ED} + \mathcal{F}_u + \mathcal{F}_\mu - \mathcal{F}_b + K_{AD} + K_{VD}) \\ E_1 - D_1 - G_{3/2}c_1 \\ -\dfrac{1}{l_2}(\mathcal{F}_u + \mathcal{F}_\mu + K_{AD} + K_{VD}) \\ -G_{5/2}c_2 + G_{3/2}c_1 \\ \vdots \\ -\dfrac{1}{l_m}(\mathcal{F}_u + \mathcal{F}_\mu - \mathcal{F}_w + K_{AD} + K_{VD}) \\ G_{M-1/2}c_M \\ -\dfrac{E_1 - D_1}{1 - p} \end{pmatrix}.$$

As with the previous section much of this work is more deeply detailed in [1]. For calculations involving eigenvalues we approximate to the maximum wave speed:

$$\lambda_\alpha^\pm = U_\alpha \pm \sqrt{gH}, \alpha = 1, 2, ..., M. \quad (17)$$

A sedimentary eigenvalue could be calculated, but it is always far surpassed by the eigenvalues in (17), so it is not used.

A. Time Integration Procedure

The domain is divided into control volumes $[x_{i-1/2}, x_{i+1/2}]$ with a uniform sizes Δx and then we divide the temporal domain into subintervals $[t_n, t_{n+1}]$ with step size Δt. We integrate (15) in space over a control volume and obtain the relation:

$$\frac{d\mathbf{W}}{dt} + \frac{F_{i+1/2} - F_{i-1/2}}{\Delta x} = \mathcal{Q}_i + \mathcal{R}_i, \quad (18)$$

where $\mathbf{W}_i(t)$ is the averaged solution $\mathbf{W}$ in the control volume C_i at time t.

$$\mathbf{W}_i(t) = \frac{1}{\Delta x}\int_{x_{i-1/2}}^{x_{i+1/2}} \mathbf{W}(t, x)dx \quad (19)$$

For computational ease, we split the equation into two steps. This enables integration in time.

$$\begin{aligned} \mathbf{W}_i^* &= \mathbf{W}_i^n + \Delta t\mathcal{R}_i^n \\ \mathbf{W}_i^{n+1} &= \mathbf{W}_i^* - \Delta t\frac{F_{i+1/2} - F_{i-1/2}}{\Delta x} + \Delta t\mathbf{Q}_i^* \end{aligned} \quad (20)$$

To determine the step size we utilise a Courant number, and in order to stabilise the solution this must be kept below one.

$$\Delta t = Cr\frac{\Delta x}{max_{\alpha=1,...,M}(|\lambda_\alpha^n|)} \quad (21)$$

As demonstrated by Audusse et al. [1], the solution is gained by reformulating the multilayer system in advective form, and then integrating it along the characteristic lines. This results in a fast and stable method that is ideal for demonstrating the multi-layered sediment problem this paper aims to overcome.

B. Discretization of the Flux Gradients

We utilise the method of characteristics to solve the advective part of the problem, and consider the equations presented in (15). Though now we consider the system in terms of 2D volumetric discharge $q_\alpha = Hu_\alpha$ thus:

$$\frac{\partial H}{\partial t} + \left(\sum_{\alpha=1}^M l_\alpha u_\alpha\right)\frac{\partial H}{\partial x} = -\sum_{\alpha=1}^M l_\alpha H\frac{\partial u_\alpha}{\partial x},$$

$$\frac{\partial(q_\alpha)}{\partial t} + u_\alpha\frac{\partial q_\alpha}{\partial x} = -q_\alpha\frac{\partial u_\alpha}{\partial x} - gH\frac{\partial(H + B)}{\partial x} - \frac{(\rho_s - \rho_w)}{2\rho_\alpha}gH^2\frac{\partial c_\alpha}{\partial x},$$

$$\frac{\partial(q_\alpha c_\alpha)}{\partial t} + u_\alpha\frac{\partial(q_\alpha c_\alpha)}{\partial x} = -H\frac{\partial u_\alpha c_\alpha}{\partial x}. \quad (22)$$

This can be re-arranged into the compact as:

$$\frac{\partial U_\alpha}{\partial t} + U_\alpha\frac{\partial U_\alpha}{\partial x} = S_\alpha(\mathbf{U}) \qquad \alpha = 0, 1, ..., M,$$

where

$$\mathbf{U} = \begin{pmatrix} H \\ q_1 \\ Hc_1 \\ q_2 \\ Hc_2 \\ \vdots \\ q_m \\ Hc_m \end{pmatrix}, \quad (23)$$

$$\mathbf{S}(\mathbf{U}) = \begin{pmatrix} -\Sigma_{\alpha=1}^M l_\alpha H\frac{\partial u_\alpha}{\partial x} \\ -Hu_1\frac{\partial u_1}{\partial x} - gH\frac{\partial}{\partial x}(H + Z) - \frac{(\rho_s - \rho_w)}{2\rho}gh^2\frac{\partial c_1}{\partial x} \\ H\frac{\partial u_1 c_1}{\partial x} \\ -Hu_2\frac{\partial u_2}{\partial x} - gH\frac{\partial}{\partial x}(H + Z) - \frac{(\rho_s - \rho_w)}{2\rho}gH^2\frac{\partial c_2}{\partial x} \\ H\frac{\partial u_2 c_2}{\partial x} \\ \vdots \\ -Hu_M\frac{\partial u_M}{\partial x} - gH\frac{\partial}{\partial x}(H + Z) - \frac{(\rho_s - \rho_w)}{2\rho}gH^2\frac{\partial c_M}{\partial x} \\ H\frac{\partial u_M c_M}{\partial x} \end{pmatrix}$$

here we define the advection velocity U_α as:

$$U_\alpha = \begin{cases} \sum_{\beta=1}^M l_\beta u_\beta, & \text{if } \alpha = 0 \\ u_\alpha, & \text{if } \alpha = 1, 2, ..., M. \end{cases} \quad (24)$$

We do not need to consider the bed Exner equation at this stage, as it is not advective. At this point the Method of Characteristics is used to impose a new grid at the next time level. It is then interpolated back to the previous time-step, enabling us to consider the characteristic curves.

$$\frac{dX_{\alpha,i+1/2}(\tau)}{d\tau} = U_{\alpha,i+1/2}(\tau, X_{\alpha,i+1/2}(\tau)), \quad (25)$$
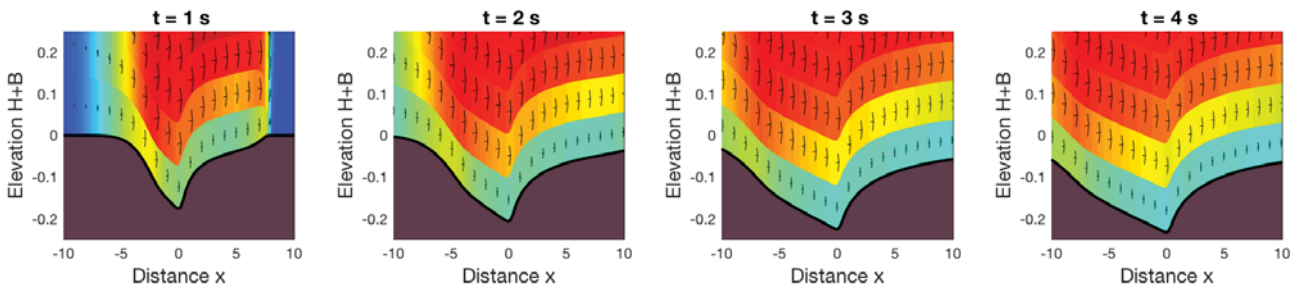$$\tau \in [t_n, t_{n+1}]$$

Integrating in time we formulate

World Academy of Science, Engineering and Technology
International Journal of Mechanical and Mechatronics Engineering
Vol:11, No:10, 2017

Fig. 3 Close up of velocity profile at $t = 1s, \ 2s, 3s \ \& \ 4s$

$$X_{\alpha,i+1/2}(t_n) =$$
$$x_{i+1/2} - \int_{t_n}^{t_n+\Delta t} U_{\alpha,i+1/2}(\tau, X_{\alpha,i+1/2}(\tau))d\tau \quad (26)$$

Thus we find the displacement between the mesh point and the next time level. We can use multiple methods to calculate the characteristic curve, but in this study we will utilise a linear polynomial.

$$\mathbf{U}_{\alpha,i+1/2}^{n+1/2} = \mathbf{U}_\alpha(t_n + \Delta t/2, x_{i+1/2}) = \widetilde{\mathbf{U}}_\alpha(t_n, X_{\alpha,i+1/2}(t_n)) \quad (27)$$

C. Discretization of the Source Terms

The characteristic solution is:

$$H_{i+1/2}^{n+1/2} = \widetilde{H}_{i+1/2}^{n+1/2} - \frac{\Delta t}{2\Delta x}\widetilde{H}_{i+1/2}^{n+1/2}\sum_{\alpha=1}^{M} l_\alpha(u_{\alpha,i+1}^{n+1/2} - u_{\alpha,i}^{n+1/2})$$

$$\begin{aligned} q_{i+1/2}^{n+1/2} = \quad & \widetilde{q}_{i+1/2}^{n+1/2} - \frac{\Delta t}{2\Delta x}(\widetilde{q}_{i+1/2}^{n+1/2}(u_{\alpha,i+1}^{n+1/2} - u_{\alpha,i}^{n+1/2}) \\ & + g\widetilde{H}_{i+1/2}^{n+1/2}((H_{i+1}^{n+1/2} + Z_{i+1}^n) - (H_i^{n+1/2} + Z_i^n)) \\ & + \frac{(\rho_s - \rho_w)}{2\rho_\alpha}gH^2(c_{i+1}^{n+1/2} - c_i^{n+1/2}) \end{aligned} \quad (28)$$

$$\begin{aligned} p_{i+1/2}^{n+1/2} = \widetilde{p}_{i+1/2}^{n+1/2} - \frac{\Delta t}{2\Delta x}\widetilde{H}_{i+1/2}^{n+1/2}(u_{\alpha,i+1}^{n+1/2}c_{\alpha,i+1}^{n+1/2} \\ - u_{\alpha,i}^{n+1/2}c_{\alpha,i}^{n+1/2}) \end{aligned}$$

where $p = Hc$

$$\begin{aligned} \widetilde{H}_{i+1/2}^{n+1/2} &= H(t_n, X_{0,i+1/2}(t_n)), \\ \widetilde{q}_{i+1/2}^{n+1/2} &= q_\alpha(t_n, X_{0,i+1/2}(t_n)) \\ \widetilde{p}_{i+1/2}^{n+1/2} &= p_\alpha(t_n, X_{0,i+1/2}(t_n)) \end{aligned} \quad (29)$$

The solutions at the characteristic foot are computed by interpolation from the departure points $X_{\alpha,i+1/2}(t_n)$. The numerical fluxes $F_{i\pm1/2}$ are calculated from the intermediate states from the predictor stage $U_{j,i\pm1/2}^{n+1/2}$.

IV. RESULTS

In this section we present the results of the benchmark dam break over a movable bed simulation. This simulation is further compared to the single-layer model, and the effects of various parts of the model are examined. We expect the model to yield smaller bottom layer fluid velocities as more layers are added: this should lead to less erosion.

In this dam break simulation, we set the domain to be $50 \ m$ long and have a flat bottom. The left hand side of the dam has a height of $3 \ m$ and the right hand side has a height of 1m. On the left side concentration is set to $c = 0.01$, and $c = 0.001$ on the right hand side . The dam break is considered to be instantaneous. The bed material, a non-cohesive sand, has a density $\rho = 1600kg/m^3$, an average particle size of $d_{50} = 0.25mm$, an erosion coefficient of 0.015, a critical shear stress of $0.0145Pa$, a porosity of $p = 0.4$, and a deposition coefficient of 0.001.

There are two points of interest in these computed results. Firstly, that there is a noticeable difference in velocity with fluid depth as highlighted in Fig. 3. This shows a clear advantage compared to standard single layered models. Secondly, the concentration coefficient, set here to 0.5 shows a good degree of diffusion up the layers, as shown in Fig. 4. As expected, this diffusion is staggered from the wave-front. Overall this simulation has shown some very encouraging results. That said, there is a non-natural spike in the bed, as shown in Fig. 3. This has two causes: firstly, the sand type is susceptible over small time frames to the creation of this artefact: secondly, and more importantly, our instantaneous dam break is not natural.

The model is a marked step away from conventional dam-break models. In order to view the impact of the assumptions made in creating this model, we compare a variety of system models in Fig. 5. We begin with the very basic fixed bed single-layer model: this shows no erosion and as a result, a further progression of the wave front. The second model is a single-layer with an erodible bed this show a greater amount of erosion than the presented model. This is expected as the bed contact velocity is higher. Finally, we compare the effects of a fixed bed and an erodible bed: in this case, there is no erosion and little further progression of the wave front, but there is a difference in velocity profile. Though the hydraulic jump is viewable in the second model (single-layer erodible bed), it is masked in the other three simulations, implying that the non-natural conditions applied stifle it.

The final comparison conducted for this study varies the number of fluid layers used. As this varies the velocity and concentration of sediment in the bottom velocity, we expect less net erosion as the number of layers are increased. As shown in Fig. 6, there is a noticeable variation in layered results that converges towards the model with 20 Layers. There
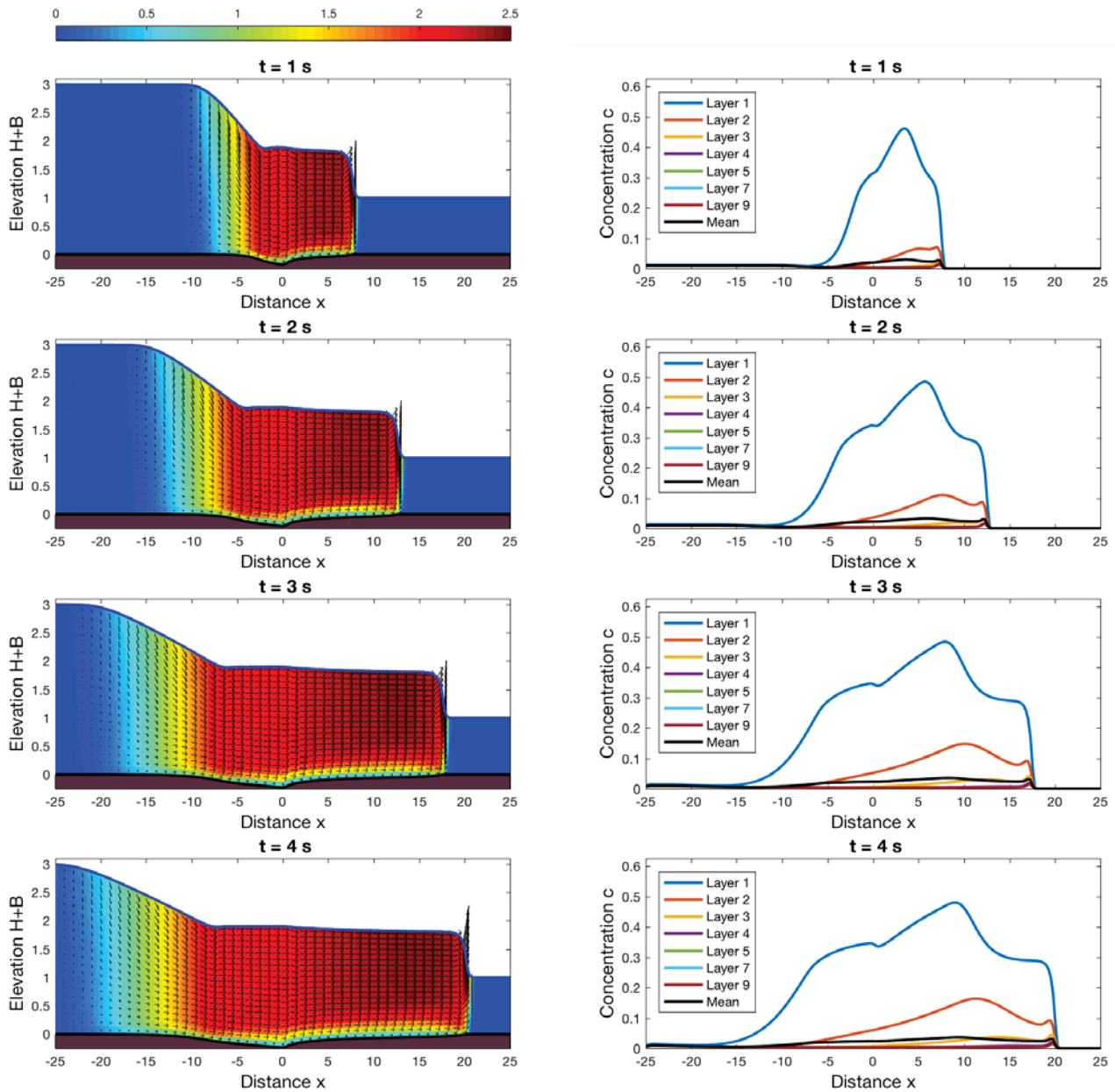
World Academy of Science, Engineering and Technology
International Journal of Mechanical and Mechatronics Engineering
Vol:11, No:10, 2017

Fig. 4 A velocity profile and concentration profile of the dam-break simulation $t = 1s, \ 2s, 3s \ and \ 84s$

is, however, a minimal effect on the fluid profile. This means that there is a greater quantity of energy in the 2 Layer system than in the 20 Layer system, this is consistent with the model design. These results validate the model and show that there is a very positive use for the multilayer system in this case.

V. CONCLUSION

A multi-layered fluid model was developed to include sediment transport over movable beds. The model was designed to include vertical diffusion of sediment between the layers to compliment the advection of sediment due to fluid flow, as it is based on the shallow water equations and has no vertical velocity component. Further the model was created as a coupled model capable of handling high sediment

concentrations and computing the effects of this on various layers.

The model was then tested against the benchmark dam break simulation. The aim of this high shear environment is to create a complex simulation that includes high sediment concentrations and a shock wave. Non-oscillatory behaviour is expected for an accurate model along with a near vertical wavefront. Both of these where achieved with this model. The model also exhibited a good variation in velocity with depth, which has a profound effect on the erosion. As shown in the results the numbers of layers in the simulation result in substantial variation of total erosion, with more layers delivering less erosion.

The model can also be used for other purposes such as recirculation and steady sediment diffusion. Very little

World Academy of Science, Engineering and Technology
International Journal of Mechanical and Mechatronics Engineering
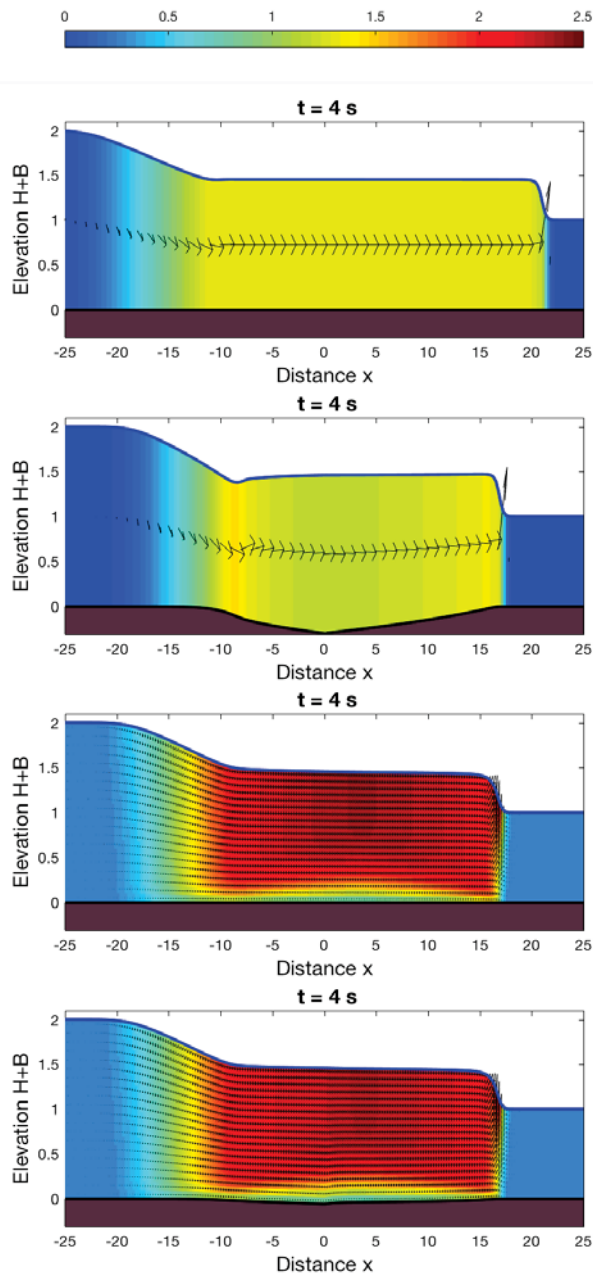Vol:11, No:10, 2017

Fig. 5 A comparison of different FVC models: single layer fixed bed, single layer erodible bed, 20 Layer fixed bed, 20 Layer erodible bed

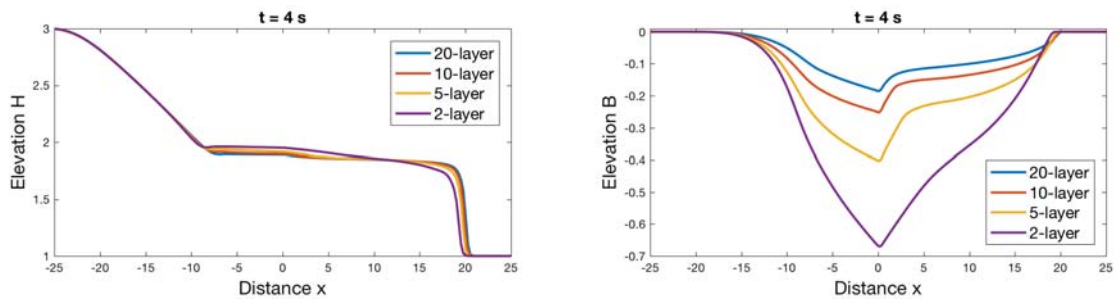Fig. 6 A comparison of the effects of varying the number of fluid layers

World Academy of Science, Engineering and Technology
International Journal of Mechanical and Mechatronics Engineering
Vol:11, No:10, 2017

literature exists on these methods as the multilayer model is required, and it has not been widely developed fo this purpose. The model could also be developed to include more robust sediment handling, with cohesive, non-cohesive sediments and multiple sediments as are often found naturally. The next area of work for this model will be development to two dimensional flow.

REFERENCES

[1] E. Audusse et al., "A fast finite volume solver for multilayered shallow water flows with mass exchange," In: *Journal of Computational Physics*, vol. 272, 2014, pp. 23-45.

[2] R. A. Bagnold, "An approach to the sediment transport problem from general physics," In: *U.S. Geological Survey Professional Paper*, 1 (1966).

[3] F. Benkhaldoun, S. Sari, and M. Seaid, "Projection finite volume method for shallow water flows," In: *Mathematics and Computers in Simulation*, vol. 118, 2015, pp. 87-101.

[4] F. Benkhaldoun et al., "Comparison of unstructured finite-volume morphodynamic models in contracting channel flows," In: *Mathematics and Computers in Simulation*, vol. 81, 2011, pp. 2081-2097.

[5] R. Briganti et al. , "An efficient and flexible solver for the simulation of morphodynamics of fast evolving flows on coarse sediments beaches," In: *International Journal for Numerical Methods in Fluids*, vol. 69, 2011, pp. 859-877.

[6] W. R. Brownlie, "Prediction of flow depth and sediment discharge in open channels," In: *Report Number KH-R-43A* Keck Laboratory of Hydraulics and Water Resources, California Institute of Technology, 1981.

[7] Z. Cao and P. Carling, "Mathematical modelling of alluvial rivers: reality and myth. Part I: General overview," In: *Water Maritime Engineering*, vol. 154, 2002, pp. 207-220.

[8] Z. Cao et al., "Computational dam-break hydraulics over erodible sediment bed," In: *Journal of Hydraulic Engineering*, vol. 67, 2004, pp. 149-152.

[9] M. J. Castro Diaz, E. D. Fernadez-Nieto, and A. M. Ferreiro, "Sediment transport models in Shallow Water equations and numerical approach by high order finite volume methods," In: *Computers and Fluids*, vol. 37, 2008, pp. 299-316.

[10] F. Engelund and J. Fredsoe, "A sediment transport model for straight alluvial channels," In: *Nordic Hydrology*, vol. 7, 1976, pp. 293-306.

[11] A. J. Grass, "Sediment Transport by Waves and Currents," In: *SERC London Cent. Mar. Technol.*, FL29, 1981.

[12] M. Guan, N. G. Wright, and P. G. Sleigh, "Multimode morphodynamic model for sediment-laden flows and geomorphic impacts," In: *Journal of Hydraulic Engineering*, vol. 141, 2015.

[13] J. Guo and P. Y. Julien, "Turbulent velocity profiles in sediment-laden flows," In: *Journal of Hydraulic Research*, vol. 39, 2001, pp. 11-23.

[14] S. Huang et al. , "Vertical distribution of sediment concentration," In: *Journal of Zhejiang University SCIENCE*, vol. 9, 2008, pp. 1560-1566.

[15] J. Hudson and P. K. Sweby, "Formations for numerically approximating hyperbolic systems governing sediment transport," In: *Journal of Scientific Computing*, vol. 19, 2003, pp. 225-252.

[16] J. Hudson and et al., "Numerical approaches for 1D morphodynamic modelling," In: *Coastal Eng*, vol. 52, 2005, pp. 691-707.

[17] J. Hudson and et al., "Numerical modeling of sediment transport applied to coastal morphodynamics," In: *Applied Numerical Mathematics*, vol. 104, 2016, pp. 30-46.

[18] X. Lui, "New Near-Wall Treatment for Suspended Sediment Transport Simulations with High Reynolds Number Turbulence Models," In: *Journal of Hydraulic Engineering*, vol. 140, 2014, pp. 333-339.

[19] X. Liu and A. Beljadid, "A coupled numerical model for water flow, sediment transport and bed erosion," In: *Computers and Fluids*, vol. 154, 2017, pp. 273-284.

[20] E. Meyer-Peter and R. Muller, "Formulas for Bed-load Transport," In: *Report on 2nd meeting on international association on hydraulic structures research*, 1948, pp. 39-64.

[21] J. Murillo and P. Garcia-Navarro, "An Exner-based coupled model for two-dimensional transient flow over erodible bed," In: *Journal of Computational Physics*, vol. 229, 2010, pp. 8704-8732.

[22] G. Rosatti and L. Fraccarollo, "A well-balanced approach for flows over mobile-bed with high sediment transport," In: *Journal of Computational Physics*, vol. 220, 2006, pp. 312-338.

[23] W. W. Rubey, "Settling velocity of gravel, sand, and silt particles," In: *American Journal of Science*, vol. 148, 1933, pp. 325-338.

[24] S. Soares-Frazao and Y. Zech, "HLLC scheme with novel wave-speed estimators appropriate for two dimensional shallow-water flow on erodible bed," In: *International Journal for Numerical Methods in Fluids*, vol. 66, 2011, pp. 1019-1036.

[25] J. Thompson et al., "Event-based total suspended sediment particle size distribution model," In: *Journal of Hydrology*, vol. 536, 2016, pp. 236-246.

[26] L. C. Van Rijn, "Sediment Pick up Functions," In: *Journal of Hydraulic Engineering*, vol. 110, 1984, pp. 1494-1502.

[27] L. C. Van Rijn, "Unified view of sediment transport by currents and waves. I: Initiation of motion, bed roughness, and bed-load transport," In: *Journal of Hydraulic Engineering*, vol. 113, 2007, pp. 649-667.

[28] V. A. Vanoni and G. N. Nomicos, "Resistance Properties of Sediment-Laden Streams," In: *Transactions of the American Society of Civil Engineers*, vol. 125, 1960, pp. 1140-1167.

[29] W. Wu and S. S. Wang, "Formulas for sediment porosity and settling velocity," In: *Journal of Hydraulic Engineering*, vol. 132, 2006, pp. 858-862.